NON-UNIFORM HEAT SOURCE AND MELTING HEAT EFFECT ON CASSON NANOFLUID FLOW OVER A RIGA PLATE IN THE PRESENCE OF NONLINEAR THERMAL RADIATION

Akaje, T. W, Olajuwon, B. I and Raji, M. T.

Department of Mathematics, Federal University of Agriculture, Abeokuta, Ogun State Nigeria

Abstract

This paper investigates the effects of a non-uniform heat source and melting heat transfer on Casson nanofluid over a Riga plate in the presence of nonlinear thermal radiation with viscous dissipation. The effects of thermophoresis and Brownian motion are also taken into account in this study. The linked non-linear partial differential equations that regulate nanofluid flow are reduced to couple non-linear ordinary differential equations using local similarity variables and then numerically solved using the Spectral Collocation technique, as shown in the current flow mathematical modelling. The effects of flow control parameters on fluid flow, temperature, and nanoparticle concentration are shown qualitatively and quantitatively. As can be seen, the results clearly show that the newly investigated factors have a significant influence on Casson fluid viscosity, thermal and chemical species transmission.

Keywords: Casson nanofluid; non-uniform heat source; Riga plate; Melting heat transfer; nonlinear thermal radiation.

1.   Introduction

An innovative research area that plays an essential role in various industrial and engineering processes, such as flow meters, MHD pump, thermal nuclear reactors, MHD generators, and the design of nuclear reactors is Casson fluid flow over a Riga plate. The applications of such flows can be found in chemical engineering, mechanical engineering, food processing, civil engineering and biomechanics. Riga plate is an electromagnetic surface in which electrodes are assembled alternatively and the arrangement generates electromagnetic hydrodynamic behaviour in the fluid flow. The first authors to introduced Riga plate are Gailitis and Leilausis [1] to generate a wall paralleled Lorentz force to control the fluid flow. Iqbal et al [2] applied Keller Box scheme and shooting technique with Runge-Kutta Fehlberg method of order 5 to investigate the effects of melting heat transport over a Riga plate. It was reported that modified Hartman number and Eckert number contribute in raising temperature. The role of heat source and thermal radiation on Casson fluid flow over a Riga plate are considered by Nasrin et al [3]. Laplace transform method was used by Asogwa et al [4] to study the impact of heat absorption and chemical reaction on Casson fluid flow over an inclined Riga plate and the study prove that chemical reaction and heat absorption parameters escalate Skin friction for both ramped and isothermal cases. At the same time, a reduction in the distribution of momentum is caused by an increase in the chemical reaction and heat absorption parameters. Naseem et al. [5] using Cattaneo-Christov model to examine third grade nanofluidic flow over a Riga plate. Loganathan and Deepa [6] considered variable chemical reaction and linear stratification on Casson fluid flow past a Riga plate. MHD Casson fluid flow over a permeable vertical Riga plate was analysed using Laplace transform method by Loganathan and Deepa [7]. Others prominent researchers who worked on Riga plate [8-10].

Heat generation and absorption is a major occurrence in industrial operations. Their presence has a substantial effect on the flow's stability. Raju et al. [11] studies the impact of chemical reaction and non-uniform heat source/sink over an unsteady inclined permeable stretching surface on Casson fluid flow and it was reported that temperature dependent heat source/sink plays a vital role on controlling the heat transfer however the surface-dependent heat source/sink also has notable influence on the heat transfer characteristics. The homotopy analysis approach is used to examine the two-dimensional magnetohydrodynamic (MHD) flow of Casson fluid across a stationary plate under non-uniform heat source/sink and Joule

Corresponding Author: Akaje T.W., Email: akajewasiu@gmail.com, Tel: +2348035568269

heating (HAM) by Ghiasi and Saleh [12]. Li et al. [13] explored shooting method to analysis numerically the significant of non-uniform heat source/sink on MHD Casson nanofluid with viscous dissipation. The result proved that the elastic parameter and heat source parameter improve the temperature profile, while the Eckert number and Casson fluid parameter degrade it. Keller Box technique was introduced to investigate the influence of non-uniform heat source/sink on stagnation point flow of an incompressible viscous fluid past a flat sheet by Krishnaiah et al. [14]. Kerur et al. [15] examine the behaviour of viscous dissipation and non-uniform heat source/sink for the Casson nanofluid over a permeable stretching sheet. It was conveyed that the presence of a non-uniform heat source/sink aids in temperature profile development. Heat generators act for positive values of the non-uniform heat source/sink parameter, while heat absorption from the boundary layer occurs for negative values of the non-uniform heat source/sink parameter. Unsteady stretching sheet with non-uniform heat source is carefully analysed numerically by Tsai et al. [16] using Chebyshev finite difference technique.

To the best of our knowledge, none of the above studies have addressed the combined effect of a non-uniform heat source/sink with melting heat on Casson nanofluid flow over a Riga plate.

2. Mathematical Formulations

The fluid flow is modelled as an incompressible two dimensional electrically conducting Casson nanofluid over a Riga-plate with non-uniform heat source/absorption. Also the behaviour of thermophoresis and Brownian motion are studied in the presence of nonlinear thermal radiation and viscous dissipation with constant value of melting temperature T_w at wall while ambient temperature and concentration are denoted by T_∞, C_∞.
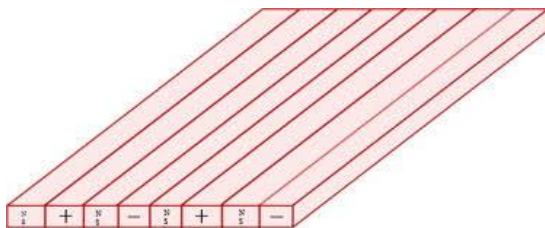

Fig. 1: Riga Plate

$$\tau_{ij} = \begin{cases} \left(\mu_B + \dfrac{p_y}{\sqrt{2\pi}}\right)2e_{ij}, & \pi > \pi_c \\ \left(\mu_B + \dfrac{p_y}{\sqrt{2\pi_c}}\right)2e_{ij}, & \pi < \pi_c \end{cases}, \quad e_{ij} = \frac{1}{2}\left(\frac{\partial u_i}{\partial x_j} + \frac{\partial u_j}{\partial x_i}\right) \tag{1}$$

Where p_y denotes fluid yield stress, μ_B defines non-Newtonian dynamical fluid viscoplastic, π describes deformation product components with self, and $\pi = e_{ij}e_{ij}, e_{ij}$ in which $(i, j)^{th}$ represents deformation module and π_c is the non-Newtonian critical based value of π.

Owing to the mentioned assumptions, the flow equation structures are presented as [17]:

$$\frac{\partial u}{\partial x} + \frac{\partial v}{\partial y} = 0 \tag{2}$$

$$u\frac{\partial u}{\partial x} + v\frac{\partial u}{\partial y} = \nu\left(1 + \frac{1}{\beta}\right)\frac{\partial^2 u}{\partial y^2} + \frac{\pi j_o M_o}{8\rho}\exp\left(\frac{-\pi}{a}y\right) \tag{3}$$

$$u\frac{\partial T}{\partial x} + v\frac{\partial T}{\partial y} = \frac{k}{\rho c_p}\frac{\partial^2 T}{\partial y^2} + \tau\left[D_B\left(\frac{\partial C}{\partial y}\frac{\partial T}{\partial y}\right) + \frac{D_T}{T_\infty}\left(\frac{\partial T}{\partial y}\right)^2\right] + \frac{\mu}{\rho c_p}\left(1 + \frac{1}{\beta}\right)\left(\frac{\partial u}{\partial y}\right)^2$$

$$+ \frac{q'''}{\rho c_p} + \frac{1}{\rho c_p}\frac{\partial q_r}{\partial y} \tag{4}$$

$$u\frac{\partial C}{\partial x} + v\frac{\partial C}{\partial y} = D_B\frac{\partial^2 C}{\partial y^2} + \frac{D_T}{T_\infty}\frac{\partial^2 T}{\partial y^2} \tag{5}$$

$$u = u_w = b\,x, \quad k\frac{\partial T}{\partial y} = \rho\left(\lambda + c_s(T_w - T_\infty)\right)v(x,0), \text{ T} = \text{T}_\infty\ C = C_\infty \text{ at } y = 0 \tag{6}$$

$$T \to T_\infty, \quad C \to C_\infty\ u \to 0, \quad \text{as} \quad y \to \infty \tag{7}$$

In the above expression where u and v indicate flow rate components along x-direction and normal to y-direction, V is the kinematic fluid viscosity, ρ is the fluid density, $\beta = \mu_B \dfrac{\sqrt{2\pi_c}}{p_y}$ is the Casson parameter, σ is the electrical conductivity of the fluid, T is the temperature, k is the thermal conductivity, c_p is the specific heat, T_w is the constant temperature at the sheet and T_∞ is the free stream temperature assumed to be constant, $\tau = \dfrac{(\rho c)_p}{(\rho c)_f}$ is the ratio of nanoparticle heat capacity and the base fluid heat capacity, D_B is the coefficient of Brownian diffusion, D_T is the coefficient of thermophoretic diffusion, M_o is magnetization of the permanents magnets mounted on the surface of Riga plate, λ the latent heat of the fluid, and a symbolizes width of magnets between electrodes.

The non-uniform heat source/sink q''' from equation (3) is model as

$$q''' = \frac{ku_w(x)}{xv}\left[A*(T_w - T_\infty)f' + (T - T_\infty)B*\right] \tag{8}$$

Where A* and B* are the coefficients of space and temperature dependent heat source/sink respectively. Here we make a note that A*>0, B*>0 corresponds to internal heat generation and A*<0, B*<0 corresponds to internal heat absorption

By means of Rosseland's approximation, q_r is define as

$$q_r = -\frac{4\sigma_s}{3k^*}\frac{\partial T^4}{\partial y} = -\frac{16\sigma_s}{3k^*}T^3\frac{\partial T}{\partial y} \tag{9}$$

in which σ and k^* are the Stefan-Boltzman constant and the mean absorption coefficient, respectively. Now Eq. (4) can be written in the form

$$u\frac{\partial T}{\partial x} + v\frac{\partial T}{\partial y} = \frac{k}{\rho c_p}\frac{\partial^2 T}{\partial y^2} + \tau\left[D_B\left(\frac{\partial C}{\partial y}\frac{\partial T}{\partial y}\right) + \frac{D_T}{T_\infty}\left(\frac{\partial T}{\partial y}\right)^2\right] + \frac{\mu}{\rho c_p}\left(1 + \frac{1}{\beta}\right)\left(\frac{\partial u}{\partial y}\right)^2$$

$$+\frac{q'''}{\rho c_p} + \frac{16\sigma_s}{3k\rho c_p}\frac{\partial}{\partial y}\left(T^3\frac{\partial T}{\partial y}\right) \tag{10}$$

With the aid of the below transformations

$$\eta = \left(\frac{u_w}{vx}\right)^{\frac{1}{2}}y, \quad \psi(x,y) = (u_w v)^{1/2}xf(\eta), \quad T = T_\infty\left(1 + (TR-1)\theta(\eta)\right), \quad \phi(\eta) = \frac{C - C_\infty}{C_w - C_\infty} \tag{11}$$

the stream function $\psi(x, y)$ is expressed such that

$$u = \frac{\partial\psi}{\partial y}, \quad v = -\frac{\partial\psi}{\partial x} \tag{12}$$

The dimensionless model becomes,

$$\left(1 + \frac{1}{\beta}\right)f''' + ff'' - f'^2 + H_a\exp(-S\eta) = 0 \tag{13}$$

$$\frac{1}{Pr}\left(1 + N_R\left(1 + (T_R - 1)\theta\right)^3\theta'\right)' + f\theta' + N_b\phi'\theta' + N_t\theta'^2 + \left(1 + \frac{1}{\beta}\right)Ec\,f''^2 \tag{14}$$

$$+ Af' + B\theta = 0$$

$$\phi'' + Lef\phi' + \frac{N_t}{N_b}\theta'' \tag{15}$$

$$\left.\begin{array}{l} f'(0) = 1, \quad Me\theta'(0) = -Pr\,f(0), \theta(0) = 1 \quad \phi(0) = 1 \\[4mm] f(\infty) = 0 \qquad \theta(\infty) = 0, \qquad \phi(\infty) = 0 \end{array}\right\} \tag{16}$$

The parameters that appeared in the above mathematical system are defined below as:

$$Pr = \frac{v}{\alpha}, Le = \frac{v}{D_B}, H_a = \frac{\pi j_o M_o v}{8\rho u_w^3 x}, Ec = \frac{u_w^2}{c_p(T_w - T_\infty)}, N_R = \frac{16\sigma_s T_\infty^3}{3kk^*}, T_R = \frac{T_w}{T_\infty}, \quad (17)$$

$$N_b = \frac{(\rho c)_p D_B (C_w - C_\infty)}{\rho c_p v}, \ N_t = \frac{(\rho c)_p D_T (T_w - T_\infty)}{\rho c_p v T_\infty}, \ S = \frac{\pi v}{au_w}, \ Me = \frac{C_f(T_w - T_\infty)}{\lambda + C_s(T_w - T_\infty)}$$

H_a is modified Hartmann number, Le is Lewis number, P_r is Prandtl number, Ec is the Eckert number, N_b and N_t respectively denote the Brownian motion and thermophoresis parameter, N_R denoted the thermal radiation parameter, T_R is the temperature ratio, S is the dimensionless parameter, Me is the melting parameter, and is expressed as the sum of Stefan number for liquid state and solid state.

The local Skin-friction C_{fx}, local Nusselt Number Nu_x, and local Sherwood Number Sh_x are presented as follows:

$$C_{fx} = \frac{\tau_w}{\rho u_w^2}, \ Nu_x = \frac{xq_w}{k(T_w - T_\infty)}, \ Sh_x = \frac{xq_m}{D_B(C_w - C_\infty)} \quad (18)$$

$$\tau_w = \left(\mu_B + \frac{p_y}{\sqrt{2\pi_c}}\right)\left(\frac{\partial u}{\partial y}\right)_{y=0}, \ q_w = -k\left(\frac{\partial T}{\partial y}\right)_{y=0} + (q_r)_w, \ q_m = -D_B\left(\frac{\partial C}{\partial y}\right)_{y=0}$$

where τ_w is the shear stress, the surface heat and mass flux q_w and q_m respectively. The dimensionless forms are

$$Re_x^{1/2}C_f = \left(1 + \frac{1}{\beta}\right)f''(0), \ \frac{Nu}{Re_x^{1/2}} = -\left(1 + Rt\left((TR-1)\theta(0)+1\right)^3\right)\theta'(0), \ \frac{Sh_x}{Re_x^{1/2}} = -\phi'(0) \quad (19)$$

$$Re_x = \frac{xu_w}{v}$$ implies the local Reynolds number.

3.   Numerical technique

To find a computational solution for the current system, the Chebyshev spectra-collocation approach is used to the differential Eqs. (13) to (15) with the boundary condition (16). Among its numerous advantages over other methods is that it has high accuracy, efficiency and ability to solve both nonlinear and linear ODEs/ PDEs systems of equations. Ehrenstein and Peyret [18] described the Chebyshev nth-order polynomial defined by $T_n(\xi); \ n \geq 0 \ as$

$$T_n(\xi) = \cos(n\cos^{-1}\xi); \qquad -1 \leq \eta \leq 1 \quad (20)$$

The recursive formula is written as $T_{n+1} = 2xT_n(x) - T_{n-1}(x); \quad n \geq 1$. the range of the flow $[0,\infty)$ is approximately taken as [0, L] in other to introduce CSCM. The far domain of the boundary is L and the value of L defines the far stream convergence of the solution. Therefore, the range [0, L] is converted to the range [-1, 1] using the following algebraic definition

$$\xi = \frac{2\eta}{L} - 1, \qquad \xi \in [-1, +1] \quad (21)$$

Let assume that $f(\eta)$, $\theta(\eta)$ and $\phi(\eta)$ is the unknown basis function $T_k(\xi)$. to be approximated.

$$\left.\begin{array}{l} f(\eta) = \sum_{k=0}^{N} a_k T_k(\eta) \\[2mm] \theta(\eta) = \sum_{k=0}^{N} b_k T_k(\eta) \\[2mm] \phi(\eta) = \sum_{k=0}^{N} c_k T_k(\eta) \end{array}\right\} \quad (22)$$

where $a_k, b_k \ and \ c_k$ are unknown coefficients to be obtained? Therefore, to have the residual equations, Eqn. (22) used on the governing equations (13) to (15), where the coefficient a_n, b_n and c_n are taken to reduce the residual error as low as possible between the considered range. Chebyshev collocation is used which is expressed according to Ehrenstein and Peyret [18].

$$\eta_j = \cos\left(\frac{\pi j}{N}\right), \qquad j = 0,...,N. \quad (23)$$

This produces a $3N+3$ set of algebraic equations along with the $3N+3$ coefficients $a_k, b_k,$ and c_k to be determined. An iterative Newton's technique following from Finlayson [19] is employed on the resulting residues $N = 30$. Hence, the boundary value algorithm is established in Mathematica software to obtain the computational results for the problem.
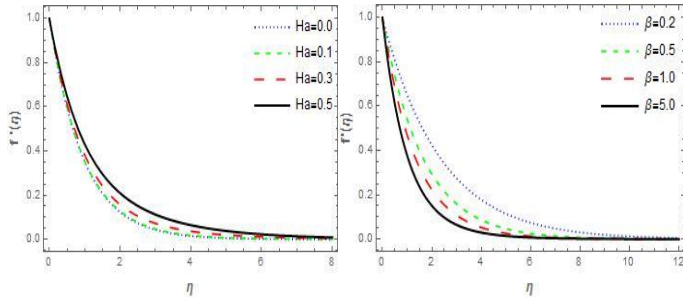

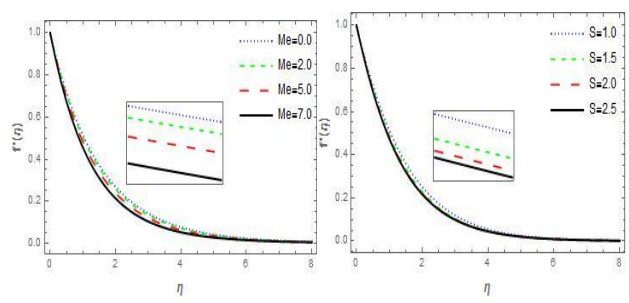Fig. 2: Influence of Ha and β on $f'(\eta)$ Fig. 3: Influence of Me and S on $f'(\eta)$
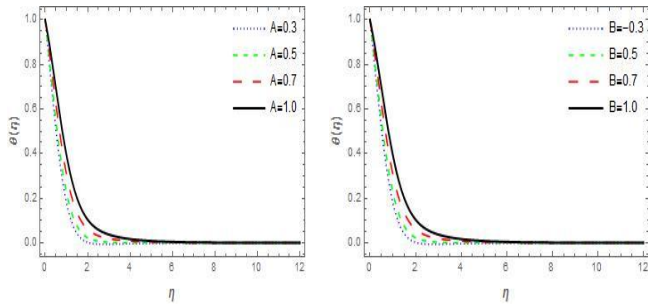

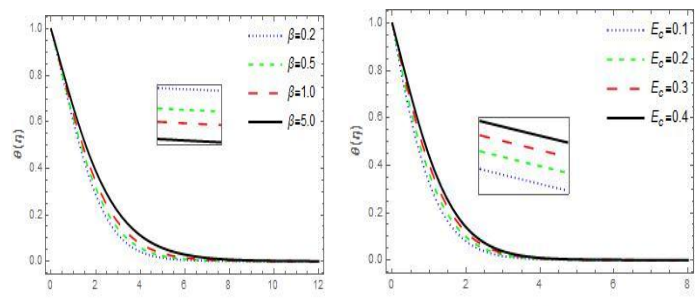Fig. 4: Influence of A and B on $\theta(\eta)$ Fig. 5: Influence of β and E_c on $\theta(\eta)$
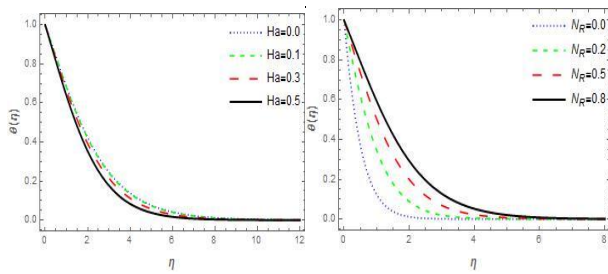

Fig. 6: Influence of Ha and N_R on $\theta(\eta)$ Fig. 7: Influence of N_t and P_r on $\theta(\eta)$
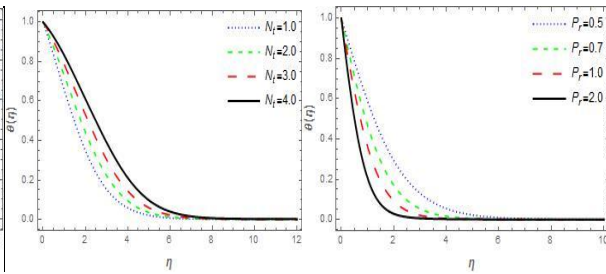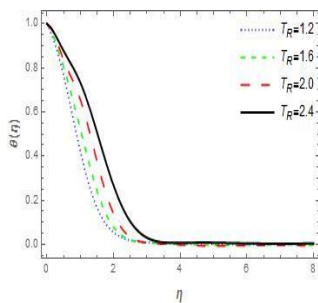
Fig. 8: Influence of T_R on $\theta(\eta)$ Fig. 9: Influence of N_b on $\phi(\eta)$ Fig. 10: Influence of Le on $\phi(\eta)$
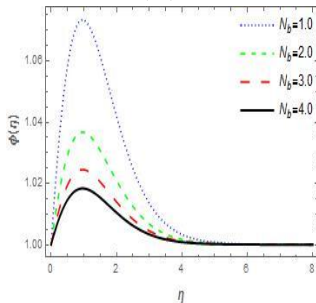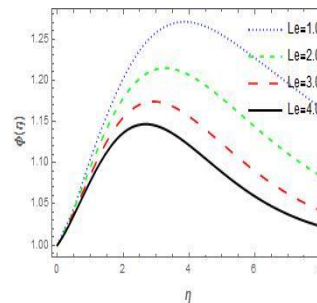
4. Discussion of Results

Numerical solutions of the boundary valued problem (10)-(14) are obtained using spectral collocation scheme and the influences of the emerging terms against the flow rate $f'(\eta)$, temperature profiles $\theta(\eta)$ and $\phi(\eta)$ dimensionless nanoparticle volume fraction. Unless

Journal of the Nigerian Association of Mathematical Physics Volume 64, (April. – Sept., 2022 Issue), 75–82
Non-Uniform Heat Source…   *Akaje, Olajuwon and Raji*   *J. of NAMP*

79

otherwise stated, in the framework of the present study the default values $H_a = 0.1, P_r = 5.0, N_R = 1.0, N_t = 0.1, T_R = 1.2, \beta = 5.0, Le = 1.0, A = 0.01, B = 0.001, E_c = 0.2, S = 0.6, Me = 1.0, N_b = 0.7$. The reaction of modified Hartmann number $\left(H_a\right)$ and Casson parameter $\left(\beta\right)$ are visualized in Figure 2. It signifies that for large values of modified Hartmann number the fluid flow rate escalates because physically $\left(H_a\right)$ results in amplifying external/internal forces like electric forces and adhesive forces etc, and under these forces, momentum of flow increases consequently the fluid flow rate enhancements, while velocity field reduce with a rise in the Casson term, this observation is in agreement with the report of Asogwa et al. [4]. Thus, flow speed magnitude is higher for Casson liquid compared to viscous liquids, and these observations are envisioned in figure [2]. The impact of melting parameter (Me) and dimensionless length parameter (S) on nanofluid velocity are depicted through figure [3]. It is noticed that large values of melting parameter enhanced the thickness of velocity boundary layer. Physically, an increase in the value of (Me) causes upsurge in the molecular motion of the fluid which enhances the flow rate and on the same figure, the variation of dimensionless parameter S on velocity film is reported to reduce the flow rate because S is the relation between viscosity and velocity of the plate with respect to width of the magnets and electrodes, therefore, increase in S leads to shrinkage in velocity distribution. The effects of non-uniform heat generation source A and B are presented in figure 4 on dimensionless temperature film, and augmentation of temperature distribution is noticed in A and B, since the heat generation source leads to a larger thermal diffusion layer that tends to upsurge the thermal boundary layer thickness Figure 5 displays the impact of Casson parameter β and Eckert number E_c on thermal fluid fields. It observed that thermal fluid field enriched with upturn in β while a rise in the heat profile with the different values of Eckert number is observed in the same figure, physically large Eckert number tends to boost the heat propagation because the fluid particles move faster along the surface since the frictional heat generation is easily noticed. The increase of modified Hartmann number $\left(H_a\right)$ showed significant effect on temperature film by decreasing the heat flow rate in figure 6, while thermal condition of the liquid and its temperature boundary sheet significantly upsurge with an increase in thermal radiation parameter in Figure 6, because the radiation term N_R describes the heat conduction contribution related to the heat radiation dispersion. The variation of temperature distribution is presented through figure 7 for different values of thermophoresis parameter N_t and Prandtl number P_r enhancement in the heat distribution as a result of an enhancement N_t is due to nanoparticles conducting strength and it is noticed that increasing in P_r reduces the heat boundary film due to huge values of Prandtl term that leads to a reduction of the fluid heat conductivity which also reduce the temperature of the fluid. Figure 8 exhibits the temperature profiles for diverse temperature ratio T_R values and thermophoresis term Nt. It is found that the heat transfer fluid and the related boundary sheet viscosity increased with up surging TR, due to the rising fluid heat transfer than the ambient heat for rising TR values that in turn raises fluid thermal state. The impact of Brownian motion Nb is illustrated in Figure 9. The concentration field is decline by an increasing Nb value. Fig. 10 shows the effects Le on the mass species transfer profiles. The mass boundary layer thickness diminished as the value of Le increases.

Journal of the Nigerian Association of Mathematical Physics Volume 64, (April. – Sept., 2022 Issue), 75–82
Non-Uniform Heat Source…   *Akaje, Olajuwon and Raji*   *J. of NAMP*

80

Table 1: Numerical results for the coefficient of wall-friction, Nusselt and concentration gradient numbers for diverse values of β, H_a, P_r, A, N_b, N_t, N_R, Me

β	H_a	P_r	N_t	N_b	A	Me	N_R	S	$-\left(1+\dfrac{1}{\beta}\right)f''$	$-\left[\left(\dfrac{(TR-1)}{\theta+1}\right)^3\right]\theta'$	$-\phi'$
0.5	0.1	5.0	0.1	0.7	0.1	1.0	1.0	0.6	-0.613405	0.375444	-0.0294
1.0									-0.759935	0.358202	-0.0300
5.0									-0.995072	0.330335	-0.0301
	0.1								-1.04115	0.304863	-0.0989
	0.3								-0.992383	0.326305	-0.1023
	0.5								-0.895451	0.359714	-0.1082
		0.7							-0.580787	0.603777	-0.1176
		1.0							-0.567085	0.786668	-0.1599
		2.0							-0.530272	1.150920	-0.2447
			1.0						-0.587212	0.312035	-0.3981
			2.0						-0.567677	0.226520	-0.4040
			3.0						-0.554004	0.165091	-0.2406
				1.0					-0.693945	0.740861	-0.1592
				2.0					-0.693946	0.740866	-0.0796
				3.0					-0.693947	0.740869	-0.0531
					0.0				-0.711897	0.879188	-0.0837
					0.5				-0.701923	0.682775	-0.0590
					1.0				-0.692138	0.487511	-0.0348
						0.1			-0.669287	0.226720	-0.0449
						0.5			-0.694336	0.250352	-0.0561
						1.0			-0.736327	0.289380	-0.0753
							0.0		-1.235110	-0.767622	1.98618
							0.2		-0.892857	1.835410	1.09168
							0.5		-0.802099	0.837695	1.06430
								1.0	-0.639225	0.299049	-0.0446
								1.5	-0.670604	0.281547	-0.0423
								2.0	-0.689586	0.273460	-0.0411

5. Conclusion

This article presents the hydromagnetic flow of the melting surface for the Casson nanofluid over a Riga plate with non-uniform heat source/sink and nonlinear thermal radiation. The solutions were numerically acquired by the spectral collocation scheme. The influence of diverse fluid terms on the fluid motion, heat diffusion and nanoparticle mass fields are discussed and graphically offered. Also, the effect of bodily terms on the skin friction, temperature gradient and mass gradient numbers are analysed and obtainable in the table. Below are the summary of our numerical results.

Enhancement of temperature field is observed when temperature ratio, thermal radiation, Eckert number, thermophoresis parameter and Casson parameter were increased.

i. Concentration profiles diminish for a higher number of melting parameters, homogeneous and heterogeneous reactions.

ii. Flow rate motion field is damped for larger melting term values, dimensionless parameter and Casson parameter

iii. The temperature boundary film tends to drop with augmented Prandtl number, non-uniform heat source/sink parameter, and modified Hartmann number $\left(H_a\right)$.

iv. The concentration distribution was enhanced with an escalation value of Lewis number.

Journal of the Nigerian Association of Mathematical Physics Volume 64, (April. – Sept., 2022 Issue), 75–82
Non-Uniform Heat Source…   *Akaje, Olajuwon and Raji*   *J. of NAMP*

81

References

[1] A. Gailitis, O. Lielausis, On a possibility to reduce the hydrodynamic resistance of a plate in an electrolyte. Appl Magnetohydrodyn Rep Phys Inst Riga 1961; 12:143–6.

[2] Z. Iqbal, E. Azhar, Z. Mehmood , E.N. Maraj, Melting heat transport of nanofluidic problem over a Riga plate with erratic thickness: Use of Keller Box scheme, Results in Physics 7 (2017) 3648–3658

[3] S. Nasrin, R. N. Monda, Md. M. Alam, Impulsively Started Horizontal Riga Plate Embedded in Unsteady Casson Fluid Flow with Rotation, Journal of Applied Mathematics and Physics, 8 (2020)1861-1876

[4] K. K. Asogwa, S. M. Bilal, I. L. Animasaun, F. M. Oudina, Insight into the significance of ramped wall temperature and ramped surface concentration: The case of Casson fluid flow on an inclined Riga plate with heat absorption and chemical reaction, Nonlinear Engineering 10 (2021) 213–230

[5] A. Naseem, A. Shafiq, L. Zhao, M.U. Farooq, Analytical investigation of third grade nanofluidic flow over a riga plate using Cattaneo-Christov model, Results in Physics 9 (2018) 961–969

[6] P. Loganathan and K. Deepa, Computational exploration of Casson fluid flow over a Riga-plate with variable chemical reaction and linear stratification, Nonlinear Analysis: Modelling and Control, 25(3) 2020, 443–460

[7] P. Loganathan and K. Deepa, Electromagnetic and radiative Casson fluid flow over a permeable vertical Riga-plate, Journal of Theoretical and Applied Mechanics 57(4), (2019) 987-998.

[8] T. Hayat, T. Abbas, M. Ayub, M. Farooq, A. Alsaedi, Flow of nanofluid due to convectively heated Riga plate with variable thickness. J Mol Liq 222 (2016) 854–62.

[9] Ahmed N, Adnan U Khan, Mohyud-Din ST. Influence of thermal radiation and viscous dissipation on squeezed flow of water between Riga plates saturated with carbon nanotubes. Coll Surf A Phys Eng Asp, 522 (2017)389–98.

[10] R. Mehmood, M. K. Nayak, N. S. Akber, O.D. Makinde. Effects of thermal-diffusion and diffusion-thermo on oblique stagnationpoint flow of couple stress Casson fluid over a stretched horizontal Riga plate with higher order chemical reaction. J. Nanofluids. 8(1) (2019) 94–102.

[11] K. V. Raju1, S.R.R. Reddy, P. B. A. Reddy, Effects Of Viscous Dissipation And Non-Uniform Heat Source/Sink On Casson Fluid Flow Over An Unsteady Inclined Permeable Stretching Surface, Int. J. Sci. Res. in Mathematical and Statistical Sciences, Vol. **5**(6), Dec 2018, ISSN: 2348-4519**.**

[12] E. K. Ghiasia, R. Saleh, 2d Flow of Casson Fluid With Non-Uniform Heat Source/Sink And Joule Heating, Frontiers in Heat and Mass Transfer (FHMT), 12, 4 (2019) Global Digital Central DOI: 10.5098/hmt.12.4

[13] Y.X. Li, M. I. U. Rehman, W.H. Huang, M. I. Khan, S. U. Khan, R. Chinram, S. Kadry, Dynamics of Casson nanoparticles with non-uniform heat source/sink: A numerical analysis, Ain Shams Engineering Journal 13 (2022) 101496

[14] M. Krishnaiah, P. Rajendar, T. V. Laxmi, M. C. K. Reddy, Influence of non-uniform heat source/sink on stagnation point flow of a MHD Casson nanofluid flow over an exponentially stretching surface, Global Journal of Pure and Applied Mathematics. ISSN 0973-1768 Volume 13, Number 10 (2017), 7009-7033.

[15] S.B. Kerur, J.V. Tawade, M. Biradar, B. K. Manvi, Effect of Non uniform heat source / Sink for the Casson nanofluid in presence of Viscous Dissipation over the porous stretching sheet, Journal of Engineering Science, 11 (7) 2020, 114-126.

[16] R. Tsai, K.H. Huang, J.S. Huang, Flow and heat transfer over an unsteady stretching surface with non-uniform heat source, International Communications in Heat and Mass Transfer 35 (2008) 1340–1343

[17] F. Mabood, K. Das, W. A. Khan, M. Khan, M. Irfan, A.S. Alshomrani, Impact of melting heat transfer and nonlinear radiative heat flux mechanisms for the generalized Burgers fluids, Results in Physics 7 (2017) 4025–4032

[18] U. Ehrenstein, R. Peyret, A Chebyshev spectral collocation method for the Navier-Stokes equations with application to double-diffusive convection. Int J Number Meth Fl. 1989;9:427–452.

[19] B.A. Finlayson, The method of weighted residuals and variational principles. New York: Academic Press; 1972.